Steel and Composite Structures, *Vol. 20, No. 5 (2016) 1023-1042*
DOI: http://dx.doi.org/10.12989/scs.2016.20.5.1023

Flexural natural vibration characteristics of composite beam considering shear deformation and interface slip

Wangbao Zhou [*1,2], Lizhong Jiang [3a], Zhi Huang [3b] and Shujin Li [2c]

[1] *School of Civil Engineering, Guangzhou University, Guangzhou, 510006, China*
[2] *School of Civil Engineering and Architecture, Wuhan University of Technology, Wuhan, 430070, China*
[3] *School of Civil Engineering, Central South University, Changsha, 410075, China*

(*Received September 15, 2015, Revised December 01, 2015, Accepted January 02, 2016*)

Abstract. Based on Hamilton's principle, the flexural vibration differential equations and boundary conditions of the steel-concrete composite beam (SCCB) with comprehensive consideration of the influences of the shear deformation, interface slip and longitudinal inertia of motion were derived. The analytical natural frequencies of flexural vibration were compared with available results previously observed by the experiments, the results calculated by the FE model and the other similar beam theories available in the open literatures. The comparison results showed that, the calculation results of the analytical and Timoshenko models had a good agreement with the results of the experimental test and FE model. Finally, the influences of shear deformation and interface slip on the flexural natural frequencies of the SCCB were discussed. The shear deformation effect increases with the increase of the mode orders of flexural natural vibration, and the flexural natural frequencies of the higher mode orders ignoring the influence of shear deformations effect would be overestimated. The interface slip effect decrease with the increase of the mode orders of flexural natural vibration, and the influence of the interface slip effect on flexural natural frequencies of the low mode orders is significant. The influence of the degree of shear connection on shear deformation effect is insignificant, and the low order modes of flexural natural vibration are mainly composed of the rotational displacement of cross sections.

Keywords: steel-concrete composite beam; shear deformation; interfacial slip; flexural natural vibration; degree of shear connection; Hamilton's principle

1. Introduction

The shear connections of the steel concrete composite beam (SCCB) attach both the concrete slab and the steel beam as a whole, so that the steel beam and the concrete slab can carry applied load together and the SCCBs can take both advantages of high compressive strength of concrete materials and the high tensile strength of steel materials. The SCCB has been widely used since last few decades because of its several advantages, such as excellent ductility, strong stiffness, and high loading capacity (Wang *et al.* 2013, Lezgy-Nazargah and Kafi 2015). In addition, SCCB

*Corresponding author, Ph.D., E-mail: zhouwangbao@163.com
[a] Ph.D., E-mail: lzhjiang@csu.edu.cn
[b] Ph.D., E-mail: huangzhi@csu.edu.cn
[c] Ph.D., E-mail: whutlsj@163.com

http://www.techno-press.org/?journal=scs&subpage=6 ISSN: 1229-9367 (Print), 1598-6233 (Online)

potentially increases the speed of construction and is eco-friendly material as it uses the recycled steel which has proven to be the promising material in the construction industry (Zhou *et al*. 2015a, b, c).

A partial composite design will result in more shear slip at the steel-concrete interface, which eventually, leads to an additional deflection. Even for a full composite design, the deflection calculated ignoring this interface slip will underestimate the deflection compared with experimental measurements (Nie *et al*. 2007, Shen *et al*. 2011). At the same time, neglect of the shear deformation of the concrete slab and steel beam such as Euler–Bernoulli beams (i.e., beams with infinite shear stiffness) might not be appropriate in some cases, e.g., for SCCBs with reduced span-to-depth ratio (Ranzi and Zona 2007, Chakrabarti *et al*. 2013). Xu and Wu (2007a, b) developed a new plane stress model of composite beams with interlayer slips, which was solved by the state space method. The research showed that the one-dimensional theory underestimated the deflection of the SCCBs due to neglect of shear deformation and the rigidity of shear connectors which significantly affected the flexural stiffness of the SCCBs if the value of rigidity located within a certain range. Therefore, the natural vibration characteristics of SCCBs are influenced by both effects of the shear deformation and interface slip. It is well known that infrastructures such as bridges, tall buildings and offshore platforms are designed for specified service lives. However, unanticipated hostile-loading environments may decrease the service life of such structures. Therefore, periodic inspection and maintenance of these structures are essential for the purpose of ensuring their healthy operational condition. The natural vibration characteristics are frequently used as diagnostic tools to detect damage in structures (Dilena and Morassi 2009, Yan and Ren 2012, Yan *et al*. 2012, Yan and Katafygiotis 2015, Yan and Ren 2015). For instance, Xia *et al*. (2007, 2008) presented a field study on condition assessment of the shear connectors in a full slab-girder bridge via vibration measurements. This study is the first attempt to detect possible damage of shear connectors in slab-girder bridges through vibration methods. Jimbo *et al*. (2012) proposed a non-destructive method for damage detection in SCCBs based on finite spectral data associated with a given set of boundary conditions.

A dynamic stiffness method was introduced by Li *et al*. (2014) to investigate the natural vibration characteristics of the SCCBs consisting of a reinforced concrete slab and a steel beam connected by the stud connectors. Based on a linear constitutive equation between the interfacial shear force and the horizontal slip, Adam *et al*. (1997) analyzed the dynamic flexural behavior of elastic two-layer beams with interlayer slip by assuming the Bernoulli-Euler hypothesis to hold for each layer separately. Berczyński and Wróblewski (2005, 2010) formulated three analytical models describing the dynamic behavior of the SCCBs: two of these were based on Euler beam theory, and one on Timoshenko beam theory. It was found out that the results obtained on the basis of the Timoshenko beam theory model achieved the highest conformity with the experimental results, both for higher and lower modes of flexural vibrations of the beam, and the frequencies of higher orders of flexural vibrations proved to be highly sensitive to damage occurring in the constructions. The research on Static, dynamic, and buckling analysis of SCCB as conducted by Xu (2007a) also verified the results of Berczyński and Wróblewski (2005, 2010). Biscontin *et al*. (2000) conducted an experiment to investigate the dynamic behavior of SCCBs subjected to small vibrations, and proposed a one-dimensional model of a SCCB where the elements connecting the steel beam and concrete slab were described by means of a strain energy density function defined throughout the beam axis. The analytical model could be used to interpret a series of dynamic tests performed on SCCBs whose connections had different linear densities. Morassi and Rocchetto (2003) conducted an experiment to investigate the changes of modal parameters of SCCBs induced by different degree of damage of shear connection under ambient vibration. The investigation revealed that: flexural frequencies showed a rather high sensitivity to damage and therefore could be considered as a valid indicator upon a diagnostic analysis. Based on Morassi's experimental investigation, Dilena and Morassi (2003) developed an Euler-Bernoulli model of a SCCB, which described the dynamic behavior of the SCCBs under damaged conditions, and a diagnostic technique was introduced to locate damages based on frequency measurements. However, the analytical model failed to take into an account of the shear deformation of cross section. In 2009, Dilena and Morassi (2009) further presented a refined model of SCCB taking into account both the shear deformation and possible vertical separation between the steel beam and the concrete slab, and conducted a comparison between the results of experimental test and those of Euler-Bernoulli model and Timoshenko model. The research results showed that the percentage errors of the Timoshenko model was less than half of those corresponding to the Euler-Bernoulli model, and the vertical separation between concrete slab and steel beam was important in case of damaged connection, even for the low vibration modes.

An analytical procedure for natural vibrations of shear-deformable two-layer beams with interlayer slip was developed by Nguyen *et al*. (2012). The effect of transverse shear flexibility of two layers was taken into account in a general way by assuming that each layer behaved as a Timoshenko beam element. Therefore, the layers had independent shear strains that depended indeed on their own shear modulus. However, the longitudinal inertia of motion was neglected in the analytical procedure. Shen and Zhong (2012) examined the natural vibrations of partial SCCBs under various boundary conditions by employing weak-form quadrature element method, which didn't consider the shear deformation of cross section, and found that the longitudinal inertia of motion could not be simply neglected in assessment of dynamic behavior of partial SCCBs. Zhou *et al*. (2013) proposed the governing differential equations of SCCBs, taking into account the influences of shear lag and interface slip on the basis of Hamilton principle. It was found that the shear lag had little influence on the period and deflection amplitude of the vibration of SCCBs.

It can be seen from these refers in the above that, only few researches on flexural natural vibration characteristics of the SCCB with comprehensive consideration of the shear deformation, interface slip and longitudinal inertia of motion were reported. In the present work, the flexural vibration equilibrium differential equations of the SCCB were derived and solved by comprehensive taking into consideration of such effects above. Then, the analytical natural frequencies of flexural vibration were compared with available results previously observed by the experiments. Finally, through 20 SCCB examples, the analytical natural frequencies of flexural vibration were compared with the results of FE model, and the effects of the degree of shear connection and shear deformation on the flexural natural frequencies of the SCCB were analyzed.

2. Section strain analysis

2.1 Basic assumptions

Qi *et al*. (2010) investigated the influences of vertical separation between the concrete slab and the steel beam on dynamic characteristics of the SCCBs without damaged connection, and their results verified that whether taking vertical separation into account or not, there was no significant influence on the natural vibration frequencies and dynamic responses of the SCCB with undamaged connection, i.e., the vertical deflections of the steel beam and concrete slab could be assumed to remain the same at any position when the vibration of the SCCB with undamaged connection is present. To simplify the calculation, the following assumptions can be used (Qi and Jiang 2010)

(1) When vibration of the SCCB is present, the vertical deflections of the steel beam and concrete slab coincide along the beam axis, namely ignoring the vertical separation between the concrete slab and steel beam.
(2) After the deformation of composite beam, the cross-sections of steel beam and concrete slab remain plane respectively.

2.2. Strain of the cross section

The sectional dimension and the coordinate system of the SCCB were shown in Fig. 1, where the position of the origin 0 of the Cartesian reference system is the barycenter of the whole cross section of the SCCB. The shear strain of the steel beam web can be expressed as

$$\gamma_{xz} = \frac{\partial w}{\partial x} - \theta = w' - \theta \tag{1}$$

The shear strain, without considering of the shear deformation, of the steel beam web can be given by

$$\gamma_{xz} = w' - \theta = 0, \qquad w' = \theta \tag{2}$$

where θ is the cross-sectional rotation angle of the SCCB; w is the vertical displacement of the SCCB.

As shown in Fig. 2, the longitudinal displacements of the cross-section of the concrete slab and steel beam are composed of the displacements produced by both the rotation of the cross-section and the relative interface slip. The longitudinal displacements, produced by cross-section rotation, of the concrete slab and steel beam can be expressed as $(z - z_c)\,\theta$ and $(z - z_s)\,\theta$ respectively, where z_c and z_s denote the z-coordinates of barycenter of the concrete slab and the steel beam respectively. The longitudinal displacements, produced by the relative interface slip, of the concrete slab and steel beam can be expressed as $k_c\xi$ and $k_s\xi$ respectively, where ξ is the longitudinal displacement difference between the barycenter of the concrete slab and steel beam. Since the self-equilibrium condition of axial forces (Zhou *et al*. 2015b), it can be concluded that

$$k_c = -A_s/A_0, \qquad k_s = A_c/(nA_0) \tag{3}$$

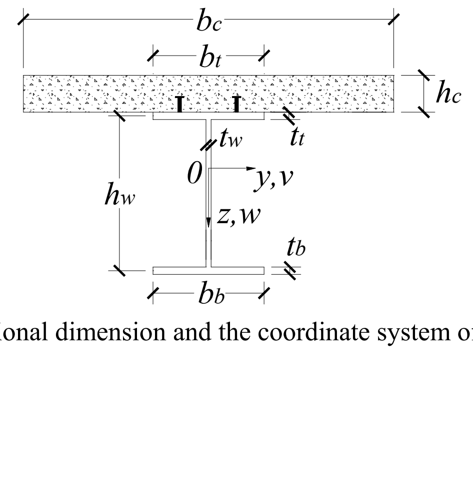

Fig. 1 Sectional dimension and the coordinate system of the SCCB

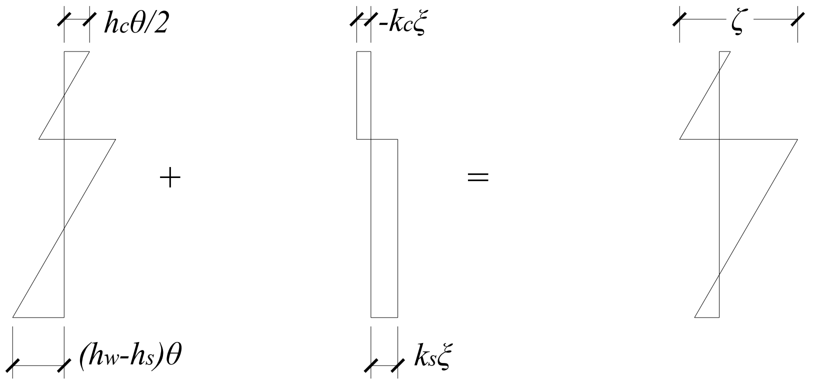

(a) Rotational displacement (b) Slip displacement (c) Total displacement

Fig. 2 Displacement mode of the cross section of the SCCB

where, $A_c = b_c h_c$; $A_s = A_t + A_b + A_w$; $A_t = b_t t_t$; $A_b = b_b t_b$; $A_w = h_w t_w$; $A_0 = A_c / n + A_S$; $n = E_s / E_c$; b_c and h_c denote the width and height of the concrete slab respectively; b_t and t_t denote the width and thickness of the upper flange of the steel beam respectively; b_b and t_b denote the width and thickness of the low flange of the steel beam respectively; h_w and t_w denote the height and thickness of the steel beam web respectively; E_s and E_c denote the Young's modulous modulus of the steel beam and concrete slab respectively.

Therefore, the longitudinal displacement of the cross-section of the concrete slab and steel beam with considering of the shear deformation effect can be expressed as

$$u_c = k_c\xi - (z - z_c)\theta, \quad u_s = k_s\xi - (z - z_s)\theta \tag{4}$$

Combining Eqs. (3) and (4), the relative interface slip between the steel beam and concrete slab with considering of the shear deformation can be given by

$$\zeta = \xi + 0.5h_c\theta + h_s\theta = \xi + h\theta \tag{5}$$

where $h = 0.5h_c + h_s$, h_s is the distance between steel beam barycenter and the interface.

Combining Eqs. (3) and (4), the longitudinal strain of the cross-section with the consideration of the shear deformation effect can be expressed as

$$\varepsilon_{cx} = k_c\xi' - (z - z_c)\theta', \quad \varepsilon_{sx} = k_s\xi' - (z - z_s)\theta' \tag{6}$$

The shear force of unit length of the interface with the consideration of the shear deformation effect is equal to

$$\varsigma = k_{sl}\zeta = k_{sl}(\xi + h\theta) \tag{7}$$

The shearing stiffness nominal value of interface between the concrete slab and steel beam can be given by (Nie *et al*. 2007)

$$k_{sl} = Kn_s / l \tag{8}$$

$$K = 0.66V_u \tag{9}$$

where, K is the shearing stiffness of single stud and the unit is N/mm; n_s is the number of studs in the same cross-section; V_u is the shear capacity of single stud; l is the longitudinal distance between any two equidistant studs.

The shear stiffness is determined by imposing that the analytical and the experimental frequencies associated to the fundamental mode coincide. The procedure is iterated until negligible changes of the two parameters are obtained in subsequent steps (Dilena and Morassi 2003, 2009). The degree of shear connection of the SCCB can be described by (Nie *et al*. 2005)

$$r = Ln_sV_u \Big/ \left(A_s f_y l\right) \tag{10}$$

where, L is the length of the SCCB; f_y is the yield strength of the steel beam.

3. Flexural natural vibration of the SCCB

3.1 Considering the effects of shear deformation

3.1.1 Flexural vibration differential equation and boundary conditions

The strain energy of the SCCB can be given by

$$V = \frac{1}{2}\int_0^L \left[\int_{A_c} E_c\varepsilon_{cx}^2 dA + \int_{A_s}\left(E_s\varepsilon_{sx}^2 + G_s\gamma_{xz}^2\right)dA + \varsigma\zeta\right]dx \tag{11}$$

Substituting Eqs. (6)-(7) to Eq. (11), it can be obtained that

$$V = \frac{1}{2}\int_0^L \left[H\xi'^2 + J\theta'^2 + k_{sl}\zeta^2 + G_sA_s\left(w' - \theta\right)^2\right]dx \tag{12}$$

$$H = E_ck_c^2A_c + E_sk_s^2A_s \tag{13}$$

$$J = E_cJ_c + E_sJ_s \tag{14}$$

$$J_c = \int_{A_c}\left(z - z_c\right)^2 dA \tag{15}$$

$$J_s = \int_{A_s}(z - z_s)^2 dA \tag{16}$$

where $G_s = 0.5E_s/(1 + \mu_s)$ is shear modulus of the steel beam; μ_s denotes the Poisson's ratio of the steel.

The total kinetic energy of the SCCB with the consideration of the longitudinal inertia of motion can be described by the following formula (Zhou *et al*. 2015b)

$$T=\frac{1}{2}\int_0^L\left(\int_{A_c}\rho_c\dot{u}_c^2dA+\int_{A_s}\rho_s\dot{u}_s^2dA\right)dx+\frac{1}{2}\int_0^L m\dot{w}^2dx \tag{17}$$

where $m = \rho_c A_c + \rho_s A_s$, ρ_c and ρ_s denote the density of the concrete and steel respectively.

Substituting Eqs. (4) and (41) into Eq. (17), it can be obtained that

$$T=\frac{1}{2}\int_0^L\left(m\dot{w}^2+H_1\dot{\xi}^2+J_1\dot{\theta}^2\right)dx \tag{18}$$

$$H_1=\rho_c k_c^2 A_c+\rho_s k_s^2 A_s \tag{19}$$

$$J_1=\rho_c J_c+\rho_s J_s \tag{20}$$

From Hamilton's principle (Morassi *et al*. 2007) , the flexural vibration differential equation and boundary conditions of the SCCB can be given by

$$H\xi^{''}-k_{sl}\zeta-H_1\ddot{\xi}=0 \tag{21}$$

$$G_sA_s\left(w^{''}-\theta^{'}\right)-m\ddot{w}=0 \tag{22}$$

$$G_sA_s\left(w^{'}-\theta\right)+J\theta^{''}-k_{sl}\zeta h-J_1\ddot{\theta}=0 \tag{23}$$

$$H\xi^{'}\delta\xi\Big|_0^L=0\,,\quad J\theta^{'}\delta\theta\Big|_0^L=0 \tag{24}$$

$$G_sA_s\left(w^{'}-\theta\right)\delta w\Big|_0^L=0 \tag{25}$$

3.1.2 Solution of the flexural natural vibration equation

For vibrations that are harmonic in time and whose frequency is ω, the displacement functions of SCCB can be considered as follows

$$\xi=\xi_1\left(x\right)\sin\left(\omega t+\varphi\right) \tag{26}$$

$$w=w_1\left(x\right)\sin\left(\omega t+\varphi\right) \tag{27}$$

$$\theta=\theta_1\left(x\right)\sin\left(\omega t+\varphi\right) \tag{28}$$

Denote that

$$D^k=\frac{\partial^k}{\partial x^k} \tag{29}$$

Substituting Eqs. (26)-(29) into Eqs. (21)-(23) ,it can be obtained that

$$\left(HD^2 - k_{sl} + H_1\omega^2\right)\xi_1 - k_{sl}h\theta_1 = 0 \tag{30}$$

$$\left(G_sA_sD^2 + m\omega^2\right)w_1 - G_sA_sD\theta_1 = 0 \tag{31}$$

$$G_sA_sDw_1 - k_{sl}h\xi_1 + \left(JD^2 + J_1\omega^2 - G_sA_s - k_{sl}h^2\right)\theta_1 = 0 \tag{32}$$

The characteristic polynomial of Eqs. (30)-(32) can be given by

$$f\left(D\right) = \begin{vmatrix} HD^2 - k_{sl} + H_1\omega^2 & 0 & -k_{sl}h \\ 0 & G_sA_sD^2 + m\omega^2 & -G_sA_sD \\ -k_{sl}h & G_sA_sD & JD^2 + J_1\omega^2 - G_sA_s - k_{sl}h^2 \end{vmatrix} \tag{33}$$

The complete primitive $(\xi_1, w_1, \theta_1)^T$ of the Eqs. (30)-(32) takes the form of

$$\left(\xi_1, w_1, \theta_1\right)^T = \sum_{i=1}^{3}\left(a_i\mathbf{C}_i\,\mathrm{e}^{D_ix} + a_{3+i}\overline{\mathbf{C}_i}\,\mathrm{e}^{\overline{D_i}x}\right) \tag{34}$$

$$\mathbf{C}_i = \left\{C_{i,1}, C_{i,2}, C_{i,3}\right\}^T = \left\{\frac{k_{sl}h}{HD_i^2 - k_{sl} + H_1\omega^2}, \frac{G_sA_wD_i}{G_sA_wD_i^2 + m\omega^2}, 1\right\}^T \quad i = 1,2,3 \tag{35}$$

where $(\bar{\cdot})$ represents the complex conjugate of $(\cdot)$, and $\{a_1, a_2,\ldots, a_6\}^T$ is a vector of constants. In Eq. (33), $\{D_i, \mathbf{C}_i\}$ is the i^{th} eigenpair of the eigenvalue problem in the x space variable. It is obtained by seeking solutions for system (30)-(32) having the form of $e^{Dx}\mathbf{C}$. The three couples of complex conjugate numbers $\{D_i, \overline{D_i}\}_{i=1}^{3}$ are the roots of characteristic polynomial $f(D)$.

The characteristic polynomial $f(D)$ is a cubic one in D^2. From fundamental mathematics, one is not difficult to figure out that there will be three real D^2 roots of $f(D)$ or one real and two complex conjugates. This property allows the representation of the exponential factors present in Eq. (34) through (cos Dx, sin Dx) harmonic functions if D^2 root of $f(D)$ is negative, through (ChDx, ShDx) hyperbolic functions if D^2 root of $f(D)$ is positive, and though suitable combination of products of harmonic and hyperbolic functions if D^2 root of $f(D)$ is complex (Biscontin *et al*. 2000, Dilena and Morassi 2003).

The common boundary conditions for the flexural natural vibration of the SCCB can be obtained from Eqs. (24)-(25) as follows

(1) The simply supported boundary conditions are

$$\xi_1^{'} = w_1 = \theta_1^{'} = 0 \tag{36}$$

(2) The clamped supported boundary condition are

$$\xi_1 = w_1 = \theta_1 = 0 \tag{37}$$

(3) The free boundary conditions are

$$\xi_1' = w_1' - \theta_1 = \theta_1' = 0 \tag{38}$$

It can be seen that there are three boundary conditions at each ends of the SCCB, and in total six boundary conditions. Then, the characteristic polynomial can be formed for the eigenvalue problem (30)-(32), by imposing that the general solution (34) must fulfill the boundary conditions listed above. In so doing, one obtains a homogeneous linear system in real constants $\{a_1, a_2,\ldots, a_6\}^T$ as follow

$$\mathbf{B}(\omega)\cdot\{a_1, a_2, \cdots, a_6\}^T = 0 \tag{39}$$

where $\mathbf{B}(\omega)$ is a 6×6 matrix depending on ω.

Natural cyclic pulsations correspond to those special ω values that cancel out the determinant of $\mathbf{B}(\omega)$

$$\left|\mathbf{B}(\omega)\right| = 0 \tag{40}$$

In order to determine the flexural natural frequencies as the roots of characteristic Eq. (40), a numerical procedure was employed, and the essential steps are similar to that presented in Refs. (Biscontin *et al*. 2000, Dilena and Morassi 2003).

3.2 Neglecting the effect of the shear deformation

The longitudinal displacement of the cross-section of the SCCB ignoring the influence of the shear deformation can be expressed as

$$u_c = k_c\xi - (z - z_c)w', \quad u_s = k_s\xi - (z - z_s)w' \tag{41}$$

Longitudinal strain at the cross section of the SCCB without considering the influence of shear deformation can be given by

$$\varepsilon_{cx} = k_c\xi' - (z - z_c)w'', \qquad \varepsilon_{sx} = k_s\xi' - (z - z_s)w'' \tag{42}$$

The longitudinal relative slip at the interface between the steel beam and concrete slab ignoring the influence of shear deformation can be described by the following expression

$$\zeta = \xi + hw' \tag{43}$$

The same as in Section 3.1, the flexural vibration equations and boundary conditions of the SCCB without considering the influence of the shear deformation can be obtained as follows

$$k_{sl}h\xi' + k_{sl}h^2w'' - Jw^{iv} - m\ddot{w} + J_1\ddot{w}'' = 0 \tag{44}$$

$$H\xi'' - k_{sl}\left(\xi + hw'\right) - H_1\ddot{\xi} = 0 \tag{45}$$

$$Jw''\delta w'\Big|_0^L = 0 \quad H\xi'\delta\xi\Big|_0^L = 0 \tag{46}$$

$$\left(k_{sl}\zeta h - Jw''' + J_1\ddot{w}'\right)\delta w\Big|_0^L = 0 \tag{47}$$

The same as in Section 3.1, the flexural natural frequencies of the SCCB can be solved.

4. Example analysis

4.1 Comparison between analytical natural frequencies of flexural vibration and the results of experimental test

To verify the accuracy of the analytical model shown in section 3, both the analytical model with boundary condition (38) and the FE model were used to analyze the flexural natural frequencies of T1PR and T1CR specimens of Refs. (Dilena and Morassi 2004, 2009). The mechanical and geometric parameters of the concrete slab and the steel beam are equal to the values shown in Table 1. The Euler-Bernoulli model and the Timoshenko model (Dilena and Morassi 2009) are also employed for those aforementioned 2 specimens. The FE analysis was carried out by using finite element program, ANSYS. The upper and low flanges and the web of the steel beam were simulated by using SHELL181 shell element. SOLID65 solid element was applied to simulate the concrete slab. The stud was simulated by COMBIN14 spring elements, the elastic modulus K of the spring element was calculated by using Eq. (9), in which the identified

Table 1 Physical parameters of the T1PR and T1CR specimens

Parameter	Value
Concrete slab	
Length L	3.50×10^3 mm
Cross-sectional area A_c	3.00×10^4 mm^2
Moment of inertia J_c	9.00×10^6 mm^4
Density (T1PR) ρ_c	2.44×10^{-9} t/mm^3
Density (T1CR) ρ	2.57×10^{-9} t/mm^3
Young's modulus E_c	4.2863×10^4 MPa
Steel beam	
Length L	3.50×10^3 mm
Cross-sectional area A_s	1.64×10^3 mm^2
Moment of inertia J_s	5.41×10^6 mm^4
Density ρ_s	7.87×10^{-9} t/mm^3
Young's modulus E_s	$2..10\times10^5$ MPa
Shearing stiffness	
Identified shearing stiffness (T1PR) k_{sl}	1.216×10^3 MPa
Identified shearing stiffness (T1CR) k_{sl}	1.963×10^3 MPa

Table 2 Comparison between experimental and analytical flexural natural frequencies

Mode	R_{EX} (Hz)	R_{FE} (Hz)	Δ_{FE} (%)	R_{EB} (Hz)	Δ_{EB} (%)	R_T (Hz)	Δ_T (%)	R_y (Hz)	Δ_y (%)
				T1CR beam					
1st	60.68	60.70	0.0	60.68	0.0	60.68	0.0	59.36	-2.2
2nd	145.46	143.17	-1.6	149.55	2.8	147.66	1.5	141.00	-3.1
3rd	247.11	244.28	-1.1	265.25	7.3	253.75	2.7	242.20	-2.0
4th	351.08	358.14	2.0	401.87	14.5	369.95	5.4	357.26	1.8
5th	461.38	483.20	4.7	553.89	20.1	492.89	6.8	484.88	5.1
				T1PR beam					
1st	60.49	60.48	0.0	60.49	0.0	60.49	0.0	59.20	-2.1
2nd	146.34	145.41	-0.6	153.23	4.7	152.04	3.9	143.86	-1.7
3rd	250.82	248.32	-1.0	275.03	9.7	266.34	6.2	247.93	-1.2
4th	361.26	361.86	0.2	418.23	15.8	391.16	8.3	364.42	0.9
5th	473.88	484.36	2.2	577.13	21.8	521.11	10.0	490.77	3.6

*Note: $\Delta_{FE} = 100\ (R_{FE} - R_{EX})/\ R_{EX}$, $\Delta_{EB} = 100\ (R_{EB} - R_{EX})/\ R_{EX}$, $\Delta_T = 100\ (R_T - R_{EX})/\ R_{EX}$, $\Delta_y = 100\ (R_y - R_{EX})/\ R_{EX}$. R_{EX} is the experimental test results. R_{FE} denotes the FE calculation results. R_{EB}, R_T and R_y denote the calculation results of the Euler-Bernoulli model, the Timoshenko model and the model proposed in this article respectively

shearing stiffness in Table 1 was employed. The vertical interactions at the interface between the concrete slab and steel beam were achieved by coupling the free degrees in the vertical direction of the nodes at the same position, i.e., ignoring the vertical separation between concrete slab and steel beam. The boundary conditions of the end of the FE models were simulated through constraining the free degrees in both the vertical and transverse directions if the end was simply supported, and through constraining the free degrees in the vertical, transverse and longitudinal directions if the end was clamped supported. There is no end boundary constraints if the end is free. The Table 2 contains a comparison between analytical natural frequencies of flexural vibration and the results of FE model and experimental test.

From Table 2, one can conclude that numerical results of the flexural natural frequencies of the FE model are consistent with the experimental test results, with no more than 5% error, verifying the validity of the FE model. The Euler-Bernoulli model, taking no account of the shearing deformation, overestimates the flexural natural frequencies and the discrepancies are even higher as the mode order rises, which shows that the influence of shear deformation effect of flexural natural frequencies becomes higher as the mode orders rises. The calculated results of Timoshenko model and the model proposed in this article, with comprehensive consideration of the influence of the shear deformation, the interface slip and longitudinal inertia of motion, agree well with the experimental test results. These results confirm the trend already observed in Ref. (Dilena and Morassi 2009).

4.2 Influence of shear deformation and interface slip on the flexural natural frequencies

Two groups of simply supported SCCBs (SCB-1, SCB-2) and two groups of clamped supported SCCBs (SCB-3, SCB-4) were selected for the analytical calculation and FE numerical simulation.

Five cases of degree of shear connection r = 0.40, 0.55, 0.70, 0.85, 1.00 were chosen for each group of the SCCBs, and the analyses of the flexural natural vibration characteristics were carried out on total 20 samples. The influences of the degree of shear connection and shear deformation on the flexural natural frequencies of the SCCBs were studied by analyzing the first five orders of the flexural natural frequencies. The mechanical and geometrical parameters of the SCCB samples

Table 3 Comparison between calculation results of the FE model and the analytical model (SCB-1)

r	Computation methods	Natural frequencies (Hz)				
		1st	2nd	3rd	4th	5th
0.40	R_{FE}	9.769	33.744	70.722	119.02	176.36
	R_y	9.548	32.941	69.86	119.51	180.46
	R_n	9.548	33.418	71.929	125.24	193.35
	e_y	-0.023	-0.024	-0.012	0.004	0.023
	e_n	-0.023	-0.010	0.017	0.052	0.096
	e_s	0.000	0.014	0.030	0.048	0.071
0.55	R_{FE}	10.104	34.519	71.631	119.93	177.23
	R_y	9.866	33.737	70.815	120.46	181.41
	R_n	9.866	34.214	72.884	126.35	194.62
	e_y	-0.024	-0.023	-0.011	0.004	0.024
	e_n	-0.024	-0.009	0.017	0.054	0.098
	e_s	0.000	0.014	0.029	0.049	0.073
0.70	R_{FE}	10.357	35.205	72.483	120.81	178.07
	R_y	10.026	34.532	71.77	121.42	182.37
	R_n	10.026	35.01	73.998	127.47	195.74
	e_y	-0.032	-0.019	-0.010	0.005	0.024
	e_n	-0.032	-0.006	0.021	0.055	0.099
	e_s	0.000	0.014	0.031	0.050	0.073
0.85	R_{FE}	10.555	35.818	73.284	121.65	178.89
	R_y	10.344	35.169	72.565	122.37	183.32
	R_n	10.344	35.646	74.793	128.58	196.85
	e_y	-0.020	-0.018	-0.010	0.006	0.025
	e_n	-0.020	-0.005	0.021	0.057	0.100
	e_s	0.000	0.014	0.031	0.051	0.074
1.00	R_{FE}	10.714	36.369	74.038	122.46	179.69
	R_y	10.503	35.646	73.361	123.33	184.12
	R_n	10.503	36.283	75.748	129.54	197.96
	e_y	-0.020	-0.020	-0.009	0.007	0.025
	e_n	-0.020	-0.002	0.023	0.058	0.102
	e_s	0.000	0.018	0.033	0.050	0.075
	C_s	0.097	0.078	0.047	0.029	0.019

Table 4 Comparison between calculation results of the FE model and the analytical model (SCB-21)

r	Computation methods	Natural frequencies (Hz)				
		1st	2nd	3rd	4th	5th
0.40	R_{FE}	6.419	22.142	46.545	79.022	118.5
	R_y	6.21	21.642	45.672	78.294	119.03
	R_n	6.21	21.801	46.467	80.84	124.6
	e_y	-0.033	-0.023	-0.019	-0.009	0.004
	e_n	-0.033	-0.015	-0.002	0.023	0.051
	e_s	0.000	0.007	0.017	0.033	0.047
0.55	R_{FE}	6.636	22.718	47.267	79.781	119.25
	R_y	6.525	22.12	46.467	79.09	119.83
	R_n	6.525	22.438	47.263	81.636	125.56
	e_y	-0.017	-0.026	-0.017	-0.009	0.005
	e_n	-0.017	-0.012	0.000	0.023	0.053
	e_s	0.000	0.014	0.017	0.032	0.048
0.70	R_{FE}	6.795	23.22	47.937	80.505	119.97
	R_y	6.684	22.597	47.104	79.885	120.62
	R_n	6.684	22.915	48.059	82.591	126.51
	e_y	-0.016	-0.027	-0.017	-0.008	0.005
	e_n	-0.016	-0.013	0.003	0.026	0.055
	e_s	0.000	0.014	0.020	0.034	0.049
0.85	R_{FE}	6.916	23.66	48.56	81.196	120.67
	R_y	6.684	23.075	47.74	80.681	121.42
	R_n	6.684	23.393	48.695	83.386	127.31
	e_y	-0.034	-0.025	-0.017	-0.006	0.006
	e_n	-0.034	-0.011	0.003	0.027	0.055
	e_s	0.000	0.014	0.020	0.034	0.049
1.00	R_{FE}	7.013	24.049	49.14	81.855	121.35
	R_y	6.843	23.552	48.377	81.318	122.06
	R_n	6.843	23.711	49.332	84.182	128.26
	e_y	-0.024	-0.021	-0.016	-0.007	0.006
	e_n	-0.024	-0.014	0.004	0.028	0.057
	e_s	0.000	0.007	0.020	0.035	0.051
	C_s	0.093	0.086	0.056	0.036	0.024

were as follows: $E_s = 2.1\times10^5$ MPa, $E_c = 3.0\times10^4$ MPa, $\mu_s = 0.3$, $\mu_c = 0.2$, $\rho_s = 7800$ kg.m^{-3}, $\rho_c = 2400$ kg.m^{-3}, $b_t = b_b = 124$ mm, $h_w = 280$ mm, $t_w = 10$ mm, $t_t = t_b = 13$ mm, $h_c = 100$ mm, $b_c = 600$ mm, $f_y = 400$ MPa, $L_1 = L_3 = 8$ m, $L_2 = L_4 = 8$ m. L_1 (i = 1, 2, 3, 4) are the calculation lengths of the 4 groups of the SCCB samples. The comparisons between analytical natural frequencies of flexural vibration and the results of FE model are as shown in Tables 3-6 and Figs. 3-5, where R_n

denotes the analytical flexural natural frequencies without consideration of the influence of the shear deformation. $e_y = (R_y - R_{FE})/ R_{FE}$ and $e_n = (R_n - R_{FE})/ R_{FE}$ denote the analytical calculation error considering influence of the shear deformation effect and that without considering such influence respectively. $e_s = (R_y - R_n)/ R_y$ denotes shear deformation effect; $C_s = (R_{FE}|_{r=1.0} - R_{FE}|_{r=0.4})/ R_{FE}|_{r=0.4}$ denotes interface slip effect.

Table 5 Comparison between calculation results of the FE model and the analytical model (SCB-3)

r	Computation methods	Natural frequencies (Hz)				
		1st	2nd	3rd	4th	5th
0.40	R_{FE}	18.95	48.717	90.308	141.45	200.17
	R_y	18.46	47.74	89.434	141.31	202.1
	R_n	18.937	50.127	96.276	157.22	232.81
	e_y	-0.026	-0.020	-0.010	-0.001	0.010
	e_n	-0.001	0.029	0.066	0.111	0.163
	e_s	0.026	0.050	0.077	0.113	0.152
0.55	R_{FE}	19.362	49.321	91.013	142.16	200.86
	R_y	18.937	48.377	90.07	142.11	202.9
	R_n	19.414	50.764	97.072	158.18	233.93
	e_y	-0.022	-0.019	-0.010	0.000	0.010
	e_n	0.003	0.029	0.067	0.113	0.165
	e_s	0.025	0.049	0.078	0.113	0.153
0.70	R_{FE}	19.727	49.881	91.683	142.86	201.54
	R_y	19.255	49.013	90.866	142.9	203.53
	R_n	19.733	51.4	98.027	159.13	234.88
	e_y	-0.024	-0.017	-0.009	0.000	0.010
	e_n	0.000	0.030	0.069	0.114	0.165
	e_s	0.025	0.049	0.079	0.114	0.154
0.85	R_{FE}	20.055	50.403	92.322	143.53	202.2
	R_y	19.574	49.491	91.502	143.54	204.33
	R_n	20.21	52.037	98.822	160.09	236
	e_y	-0.024	-0.018	-0.009	0.000	0.011
	e_n	0.008	0.032	0.070	0.115	0.167
	e_s	0.032	0.051	0.080	0.115	0.155
1.00	R_{FE}	20.349	50.892	92.933	144.17	202.85
	R_y	19.892	50.127	92.139	144.18	204.97
	R_n	20.528	52.674	99.618	161.04	236.95
	e_y	-0.022	-0.015	-0.009	0.000	0.010
	e_n	0.009	0.035	0.072	0.117	0.168
	e_s	0.032	0.051	0.081	0.117	0.156
C_s		0.074	0.045	0.029	0.019	0.013

Table 6 Comparison between calculation results of the FE model and the analytical model (SCB-4)

r	Computation methods	Natural frequencies (Hz)				
		1st	2nd	3rd	4th	5th
0.40	R_{FE}	12.449	32.141	60.127	95.267	136.52
	R_y	12.094	31.35	59.039	94.208	136.22
	R_n	12.253	32.304	62.062	101.21	149.9
	e_y	-0.029	-0.025	-0.018	-0.011	-0.002
	e_n	-0.016	0.005	0.032	0.062	0.098
	e_s	0.013	0.030	0.051	0.074	0.100
0.55	R_{FE}	12.759	32.622	60.711	95.882	137.14
	R_y	12.413	31.827	59.675	94.844	136.86
	R_n	12.572	32.941	62.699	102.01	150.7
	e_y	-0.027	-0.024	-0.017	-0.011	-0.002
	e_n	-0.015	0.010	0.033	0.064	0.099
	e_s	0.013	0.035	0.051	0.076	0.101
0.70	R_{FE}	13.028	33.064	61.263	96.474	137.73
	R_y	12.731	32.304	60.312	95.481	137.49
	R_n	12.89	33.418	63.336	102.8	151.5
	e_y	-0.023	-0.023	-0.016	-0.010	-0.002
	e_n	-0.011	0.011	0.034	0.066	0.100
	e_s	0.012	0.034	0.050	0.077	0.102
0.85	R_{FE}	13.265	33.471	61.785	97.043	138.31
	R_y	12.89	32.782	60.789	96.117	137.97
	R_n	13.108	33.896	63.972	103.44	152.29
	e_y	-0.028	-0.021	-0.016	-0.010	-0.002
	e_n	-0.012	0.013	0.035	0.066	0.101
	e_s	0.017	0.034	0.052	0.076	0.104
1.00	R_{FE}	13.476	33.85	62.28	97.592	138.88
	R_y	13.208	33.1	61.267	96.754	138.61
	R_n	13.367	34.373	64.609	104.23	153.09
	e_y	-0.020	-0.022	-0.016	-0.009	-0.002
	e_n	-0.008	0.015	0.037	0.068	0.102
	e_s	0.012	0.038	0.055	0.077	0.104
	C_s	0.082	0.053	0.036	0.024	0.017

Fig. 3 shows the analytical calculation errors between the flexural natural frequencies of 4 groups of SCCBs considering the influence of the shear deformation and those without considering such effect. It can be seen from Fig.3 that, the analytical calculation results have a great agreement with the numerical calculation results of flexural natural frequencies when the shear deformation, interface slip and longitudinal inertia of motion are considered comprehensively.

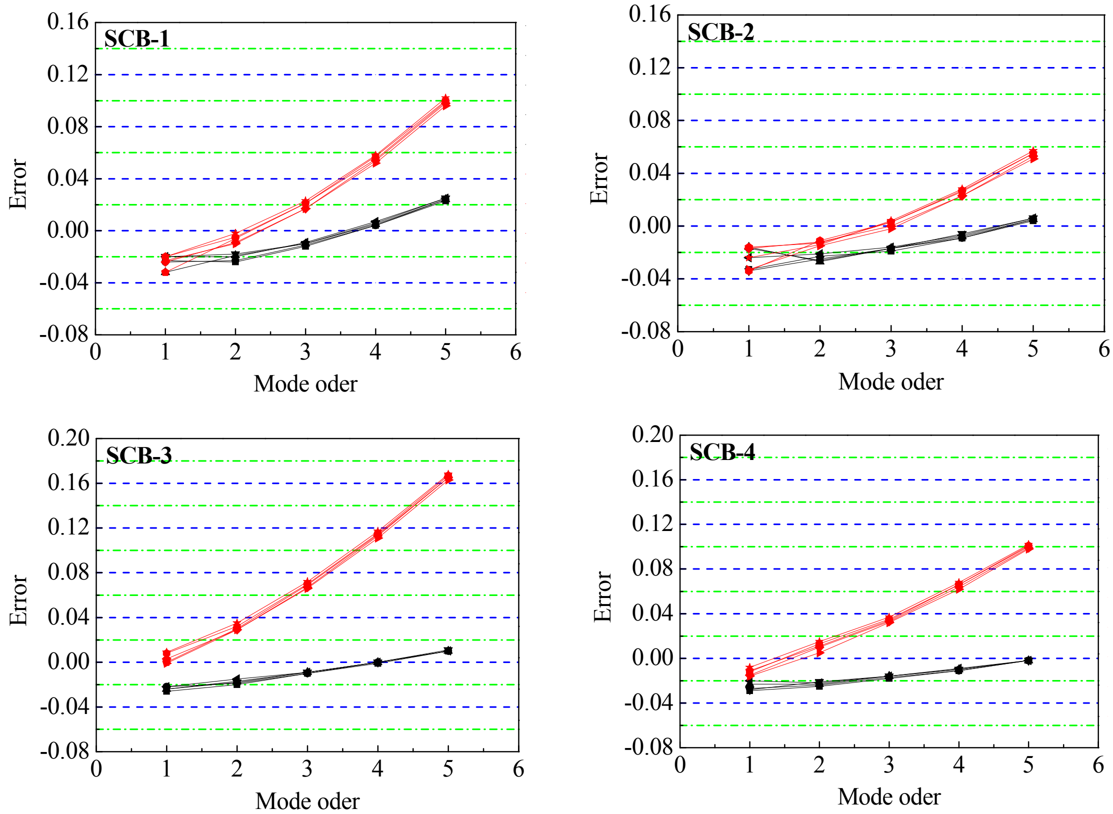

Fig. 3 Relationship between the calculation errors and the mode orders of flexural natural vibration (The red and the black dashed lines represent the calculation errors without considering the influence of shear deformation and those considering such influence respectively)

The calculation error e_y is less than 4%, verifying the validity of the analytical calculation model as derived in this article. When the influence of shear deformation of the SCCBs is not taken into account, the analytical calculation error e_n of the flexural natural frequencies of the higher mode orders exceeds 16%, and the flexural natural frequencies are greatly overestimated, indicating that the influence of shear deformation on the flexural natural frequencies of the higher mode orders should not be neglected.

Fig. 4 shows the relationship between shear deformation effects e_s and the mode orders of the flexural natural vibration. The shear deformation effect e_s increases as the mode order of flexural natural vibration rises. It can be seen from Fig. 4 that, the shear deformation effect e_s is very small in low mode orders of flexural natural vibration. This indicates that the modes of low orders are mainly composed of the cross-sectional rotational displacement, and with almost no shear deformation. The shear deformation effect e_s of high mode orders of flexural natural vibration is close to 16%, i.e., the calculation results of the flexural natural frequencies of the higher mode orders would be greatly overestimated when the influence of shear deformation effect is not considered. The influence of the degree of shear connection on the shear deformation effect e_s of the flexural natural vibration is insignificant. The reason is that the steel beam web bears most of the vertical shear of SCCBs, which doesn't have much to do with the degree of shear connection.

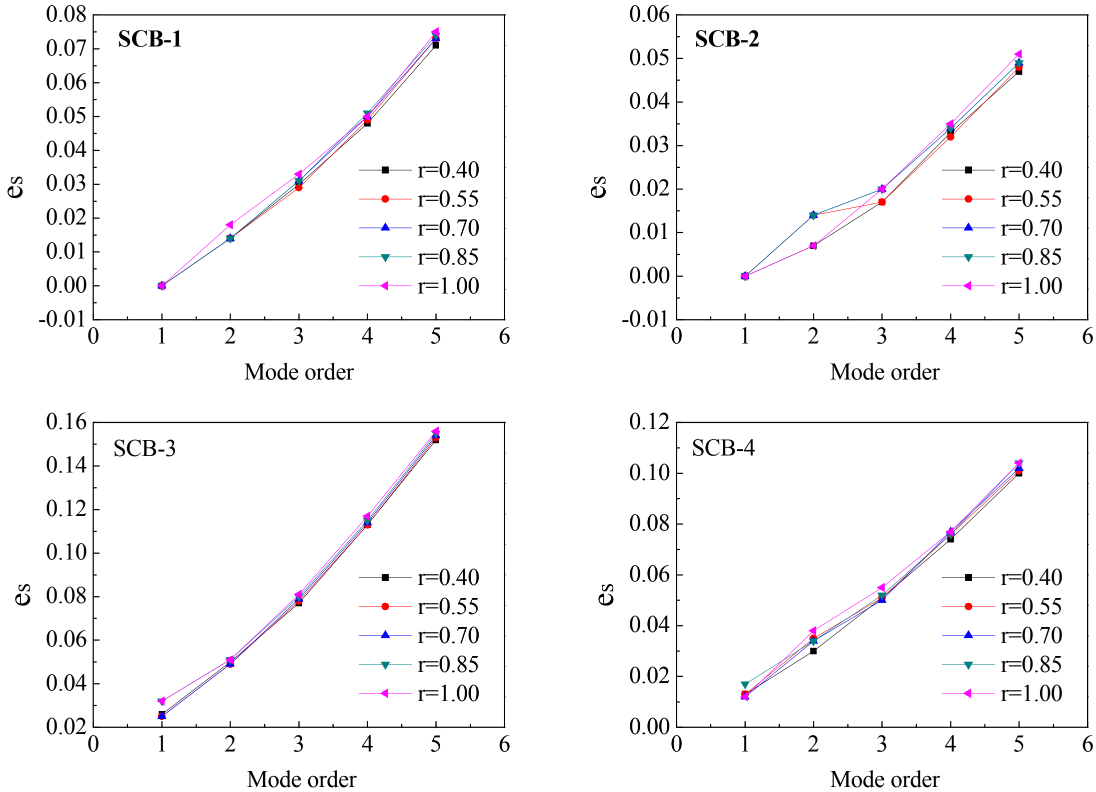

Fig. 4 Relationship between the shear deformation effect and the mode orders of flexural natural vibration

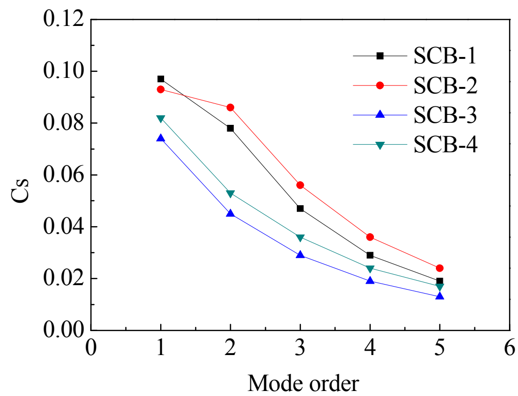

Fig. 5 Relationship between the interface slip effect and the mode orders of flexural natural bibration

The moment of inertia of the cross-section of the SCCB increased with the increase of interface shearing stiffness between the concrete slab and steel beam, and the modes of the low orders of the flexural natural vibration are dominated by the cross-sectional rotation deformation (Nie *et al*. 2004, Nie *et al*. 2005). Therefore, the interface shearing stiffness has a great influence on flexural natural frequencies of the low mode orders and the flexural natural frequencies of the SCCB increases with the increase of the shearing stiffness of the interface. Fig.5 shows the relationship between the interface slip effect C_s and the mode orders of flexural natural vibration. The interface slip effect C_s decreases with the increase of the mode orders, and gthe effect of interface slip C_s is close to 10% at low mode orders. This indicates that the influence of interface slip effect on the flexural natural frequencies of the low mode orders should not be neglected.

5. Conclusions

The moment of inertia of the cross-section of the SCCB increased with the increase of interface shearing stiffness between the concrete slab and steel beam, and the modes of the low orders of the flexural natural vibration are dominated by the cross-sectional rotation deformation (Nie *et al*. 2004, Ni *et al*. 2005). Therefore, the interface shearing stiffness has a great influence on flexural natural frequencies of the low mode orders and the flexural natural frequencies of the SCCB increases with the increase of the shearing stiffness of the interface. Fig. 5 shows the relationship between the interface slip effect C_s and the mode orders of flexural natural vibration. The interface slip effect C_s decreases with the increase of the mode orders, and the effect of interface slip C_s is close to 10% at low mode orders. This indicates that the influence of interface slip effect on the flexural natural frequencies of the low mode orders should not be neglected.

Acknowledgments

The research described in this paper was financially supported by the National Natural Science Function of China (51408449, 51378502) and the Fundamental Research Funds for the Central Universities of China (2014-IV-049).

References

Adam, C., Heuer, R. and Jeschko, A. (1997), "Flexural vibrations of elastic composite beams with interlayer slip", *ACTA Mech*., **125**(1), 17-30.

Berczyński, S. and Wróblewski, T. (2005), "Vibration of steel-concrete composite beams using the Timoshenko beam model", *J. Vib. Control*., **11**(6), 829-848.

Berczyński, S. and Wróblewski, T. (2010), "Experimental verification of natural vibration models of steel-concrete composite beams", *J. Vib. Control*., **16**(14), 2057-2081.

Biscontin, G., Morassi, A. and Wendel, P. (2000), "Vibrations of steel-concrete composite beams", *J. Vib. Control*., **6**(5), 691-714.

Chakrabarti, A., Sheikh, A.H., Griffith, M. and Oehlers, D.J. (2013), "Dynamic response of composite beams with partial shear interaction using a higher-order beam theory", *J. Struct. Eng*., **139**(1), 47-56.

Dilena, M. and Morassi, A. (2003), "A damage analysis of steel-concrete composite beams via dynamic methods: Part II. Analytical models and damage detection", *J. Vib. Control*., **9**(5), 529-565.

Dilena, M. and Morassi, A. (2004), "Experimental modal analysis of steel concrete composite beams with partially damaged connection", *J. Vib. Control*., **10**(6), 897-913.

Dilena, M. and Morassi, A. (2009), "Vibrations of steel-concrete composite beams with partially degraded connection and applications to damage detection", *J. Sound. Vib*., **320**(1), 101-124.

Jimbo, S., Morassi, A., Nakamura, G. and Shirota, K. (2012), "A non-destructive method for damage detection in steel-concrete structures based on finite eigendata", *Inverse Probl. Sci. Eng*., **20**(2), 233-270.

Lezgy-Nazargah, M. and Kafi, L. (2015), "Analysis of composite steel-concrete beams using a refined high-

order beam theory", *Steel Compos. Struct, Int. J.*, **18**(6), 1353-1368.
Li, J., Huo, Q., Li, X., Kong, X. and Wu, W. (2014), "Dynamic stiffness analysis of steel-concrete composite beams", *Steel Compos. Struct, Int. J.*, **16**(6), 577-593.
Morassi, A. and Rocchetto, L. (2003), "A damage analysis of steel-concrete composite beams via dynamic methods: Part I. Experimental results", *J. Vib. Control*, **9**(5), 507-527.
Morassi, A., Nakamura, G., Shirota, K. and Sini, M. (2007), "A variational approach for an inverse dynamical problem for composite beams", *Eur. J. Appl. Math.*, **18**(1), 21-55.
Nguyen, Q., Hjiaj, M. and Le Grognec, P. (2012), "Analytical approach for free vibration analysis of two-layer Timoshenko beams with interlayer slip", *J. Sound. Vib.*, **331**(12), 2949-2961.
Nie, J., Fan, J. and Cai, C.S. (2004), "Stiffness and deflection of steel-concrete composite beams under negative bending", *J. Struct. Eng.*, **130**(11), 1842-1851.
Nie, J., Cai, C.S. and Wang, T. (2005), "Stiffness and capacity of steel-concrete composite beams with profiled sheeting", *Eng. Struct.*, **27**(7), 1074-1085.
Nie, J.G., Cai, C.S., Zhou, T.R. and Li, Y. (2007), "Experimental and analytical study of prestressed steel-concrete composite beams considering slip effect", *J. Struct. Eng.-ASCE*, **133**(4), 530-540.
Qi, J. and Jiang, L. (2010), "Effects of interface slip and semi-rigid joint on elastic seismic response of steel-concrete composite frames", *J. Central South Univ. Technol.*, **17**(6), 1327-1335.
Qi, J., Jiang, L., Zhang, C. and Yu, Z. (2010), "Effects of interface slip, vertical uplift and shear deformation on dynamic behavior of steel-concrete composite continuous beams", *J. Central South Univ.* (*Sci. Technol.*), **41**(6), 2334-2343.
Ranzi, G. and Zona, A. (2007), "A steel-concrete composite beam model with partial interaction including the shear deformability of the steel component", *Eng. Struct.*, **29**(11), 3026-3041.
Shen, Z. and Zhong, H. (2012), "Static and vibrational analysis of partially composite beams using the weak-form quadrature element method", *Math. Probl. Eng.*, **2012**, 1-23.
Shen, X., Chen, W., Wu, Y. and Xu, R. (2011), "Dynamic analysis of partial-interaction composite beams", *Compos. Sci. Technol.*, **71**(10), 1286-1294.
Wang, W., Li, Q., Zhao, C. and Zhuang, W. (2013), "Dynamic properties of long-span steel-concrete composite bridges with external tendons", *J. Highway Transport. Res. Develop.*, **7**(4), 30-38.
Xia, Y., Hao, H. and Deeks, A.J. (2007), "Dynamic assessment of shear connectors in slab-girder bridges", *Eng. Struct.*, **29**(7), 1475-1486.
Xia, Y., Hao, H., Deeks, A.J. and Zhu, X. (2008), "Condition assessment of shear connectors in slab-girder bridges via vibration measurements", *J. Bridge Eng.*, **13**(1), 43-54.
Xu, R. and Wu, Y. (2007a), "Static, dynamic, and buckling analysis of partial interaction composite members using Timoshenko's beam theory", *Int. J. Mech. Sci.*, **49**(10), 1139-1155.
Xu, R. and Wu, Y. (2007b), "Two-dimensional analytical solutions of simply supported composite beams with interlayer slips", *Int. J. Solid. Struct.*, **44**(1), 165-175.
Yan, W. and Katafygiotis, L.S. (2015), "A two-stage fast Bayesian spectral density approach for ambient modal analysis. Part I: Posterior most probable value and uncertainty", *Mech. Syst. Signal. Process.*, **54-55** 139-155.
Yan, W. and Ren, W. (2012), "Operational modal parameter identification from power spectrum density transmissibility", *Comput-Aided Civ. Infra. Eng.*, **27**(3), 202-217.
Yan, W. and Ren, W. (2015), "An Enhanced Power Spectral Density Transmissibility (EPSDT) approach for operational modal analysis: Theoretical and experimental investigation", *Ent. Struct.*, **102**, 108-119.
Yan, W., Ren, W. and Huang, T. (2012), "Statistic structural damage detection based on the closed-form of element modal strain energy sensitivity", *Mech. Syst. Signal. process.*, **28**, 183-194.
Zhou, W., Jiang, L. and Yu, Z. (2013), "Analysis of free vibration characteristic of steel-concrete composite box-girder considering shear lag and slip", *J. Central South Univ.*, **20**(9), 2570-2577.
Zhou, W., Jiang, L., Li, S. and Kong, F. (2015a), "Elastic distortional buckling sanalysis of I-steel concrete composite beam considering shear deformation", *Int. J. Struct. Stab. Dy.*, 1550045.
Zhou, W., Li, S., Jiang, L. and Qin, S. (2015b), "Vibration analysis of steel-concrete composite box beams considering shear lag and slip", *Math Probl. Eng.*, **2015**(1), 1-8.

Zhou, W., Li, S., Jiang, L. and Zhi, H. (2015c), "Distortional buckling calculation method of steel-concrete composite box beam in negative moment area", *Steel Compos. Struct, Int. J.*, **19**(5), 1203-1219.

CC